Glassy Conformations in Wrinkled Membranes

Sahraoui Chaieb,[1,2,*] Vinay K. Natrajan,[2] and Ahmed Abd El-rahman[2]

[1]*Mechanical Engineering Department, University of Illinois at Urbana-Champaign, Urbana, Illinois 61801, USA*

[2]*Beckman Institute for Advanced Science and Technology, University of Illinois at Urbana-Champaign, Urbana, Illinois 61801, USA*

(Received 28 October 2004; published 21 February 2006)

Partially polymerized membranes display a striking mechanical transition at low temperature known as the wrinkling transition. Fluorescence and scanning electron microscopy as well as profile measurements using an atomic force microscope revealed the existence of three degrees of wrinkling depending on the degree of the membrane polymerization. At low polymerization the membrane undergoes a cascade of wrinkling to form a folded phase with a characteristic exponent η equal to 3, at intermediate polymerization, the membrane is in an intermediate-wrinkled phase (similar to the crumpling of an elastic sheet) with $\eta \sim 2.5$, while at high polymerization the membrane undergoes an abrupt ''compaction'' to the wrinkled-rough phase with $\eta \sim 2$.

DOI: 10.1103/PhysRevLett.96.078101 PACS numbers: 87.16.Dg, 64.60.Fr, 68.55.Jk, 87.15.La

The large deformations of a regular sheet of paper, when crumpled inside the palm of a hand, generate an irregular network of creases and ridges. If the operation is repeated, the structure of the ridges and singularities becomes more uniform and scale independent [1,2]. In spite of the extensive work on large deformations and crumpling of elastic sheets, the mechanisms that drive the formation of such patterns are still unclear and so are the kinematics of such morphological transformation [1,3,4].

Unlike large-scale elastic sheets, and similar to polymers, thermally fluctuating membranes assume folded and collapsed conformations as a result of a competition between entropy and elasticity [5,6]. Most studies have focused on tethered membranes [7]. Examples of real-life tethered membranes are the skeleton of red blood cells (RBC) [8], molybdenum sulfide sheets [9], and graphite oxide (GO). Unlike polymers, however, tethered membranes exhibit a low-temperature flat phase characterized by a long-range orientational order [6]. A transition between this flat phase and a crumpled phase has been predicted theoretically but not observed in computer simulations, for dimensional space smaller than 4, probably due to the implemented self-avoidance interactions that favor a flat phase [10–12]. Few experiments have attempted to show evidence of the existence of both the flat phase and the crumpled phase. By measuring a roughness exponent, light and x-ray scattering revealed a flat phase in the RBC cytoskeleton [13]. On the other hand, GO membranes were reported to exhibit a crumpled conformation in a good solvent and a compact conformation in a bad solvent [14], but the results were inconclusive since the large persistence length of GO membranes hinders the occurrence of a crumpled phase [15].

In contrast to fixed connectivity membranes, partially polymerized membranes made of diacetylenic phospholipids exhibit a remarkable low-temperature wrinkled phase [16] characterized by randomly frozen normals [17–19] distinct from the high-temperature crumpled phase where the normals fluctuate in time [6]. This transition from a fluctuating vesicle at high temperature to a wrinkled membrane at low temperature might be due to the randomness created in the local curvature of the membrane after polymerization [17]. Furthermore, it has been argued that this *partial* polymerization generates a quenched-in disorder [17,18,20,21] in the form of grain boundaries between quenched-in dislocations [19] or randomness in the elastic properties of the membranes [21] or in the spontaneous curvature [16,22]. It was further assumed that this low-temperature phase is an analog to a spin-glass phase in magnetic systems [21] driven by frustration [18] where a ''roughened'' glassy phase with a roughness exponent different from that for systems with no defects may appear and where the roughness would be coupled to the disorder created after polymerization [20]. Here we report a discovery of a folding transition at low polymerization, as well as multiple ''phases'' characterized by different roughness exponents depending on the degree of polymerization of the membrane. These wrinkling phases are similar to glass phases in jammed granular materials and colloidal suspensions, where the built-up geometrical constraints restrict the system's access to the phase space [23].

We use polymerizable lipids [1,2-bis(10,12-tricosadiynoyl)-*sn*-glycero-3-phosphocholine] purchased from Avanti Lipids in powder or dissolved in chloroform and stored at $-20\,^{\circ}\mathrm{C}$. These lipids have triple bonds in their aliphatic tails that can be photopolymerized. When spherical vesicles, made of these lipids, are cooled, they undergo a shape transformation to helical ribbons at the chain melting temperature T_m, which is around $37\,^{\circ}\mathrm{C}$ upon cooling and $43\,^{\circ}\mathrm{C}$ when heating. This transformation is thought to be due to the chirality of these lipids [24] although weakly [25]. In the present experiment vesicles are prepared in the high-temperature phase. Large unilamellar vesicles were prepared using electroformation: We dissolve the lipids in chloroform and brush the solution on the electrodes, which we store in vacuum overnight for the solvent to evaporate. The electrodes biased at a 10 V/10 Hz ac are then dipped in pure water at $50\,^{\circ}\mathrm{C}$

and left for 1–3 h for the vesicles to grow to a size of 10–100 μm. Small unilamellar vesicles of uniform sizes ranging from 100 to 500 nm are made via extrusion of larger vesicles. We cool the vesicles below T_m and polymerize the aliphatic tails by exposing them to uv radiation at 254 nm, which breaks the multiple bonds of the aliphatic tails and creates new covalent bonds between the various lipid molecules. We then heat the vesicles to 50 °C, whereupon they become spherical. The cooled vesicles wrinkle at a temperature $T_w \ll T_m$. To characterize the transition, we used two-photon confocal scanning fluorescence microscopy and the fluorescent amphiphilic molecule (Laurdan) as the probe, which, when excited by a two-photon 770 nm, has an emission spectrum centered around 449 nm (blue) when the membrane is in the low-temperature gel phase and centered around 499 nm (green) when the membrane is in the high-temperature liquid crystalline phase. The transition is characterized by the change in the sign of the generalized polarization defined as $\mathrm{GP} = (I_g - I_l)/(I_g + I_l)$, where I_g and I_l are the intensities at the maximum emission wavelengths in the gel phase and the liquid crystalline phase [26].

When partially polymerized vesicles are cooled, the change in the GP occurs at the nucleation of the first folds. The transition temperature corresponds to the jump in the GP value (data not shown). Surprisingly, after polymerization, the jump at 37 °C disappears, and instead a jump in the GP value appears at lower temperatures corresponding to the wrinkling transition (T_w). Because this transition involves a folding process, T_w is defined as the temperature at onset. The ''unwrinkling'' may take an order of magnitude longer, depending on the polymerization.

The wrinkling process depends on the amount of polymer network created in the vesicle's bilayer (Fig. 1). Let ϕ be the degree of polymerization measured using absorption spectra of the polymer created. At low polymerization ($\phi < 10\%$), the cooled vesicle undergoes a folding cascade in the form of a succession of large creases. Each crease is of the order of the vesicle's size. When ϕ is increased, a pattern of smaller creases takes place (Fig. 2). At higher ϕ, the wrinkling was so sudden that we were not able to record any type of folding cascade. The floppy vesicle jumps abruptly to a compacted and rigid structure (Fig. 1).

Wrinkling is accompanied by surface roughening [2,20,27]. The surface topography was investigated using a tapping-mode atomic force microscope (AFM). The radius of the Si tip is about 10 nm, and the side angle is about 10°. Repeated scans with a small force set point less than 1 nN were carried out in order to ensure no obvious distortion caused by tip-sample interaction. The vesicles of sizes ranging from 300 nm to 40 μm are cooled in the aqueous solution and then transferred to a substrate to be scanned. In the case of vesicles larger than 10 μm, we use a scanning window of the order of 10 μm, which is the maximum lateral distance the AFM scanner can achieve.

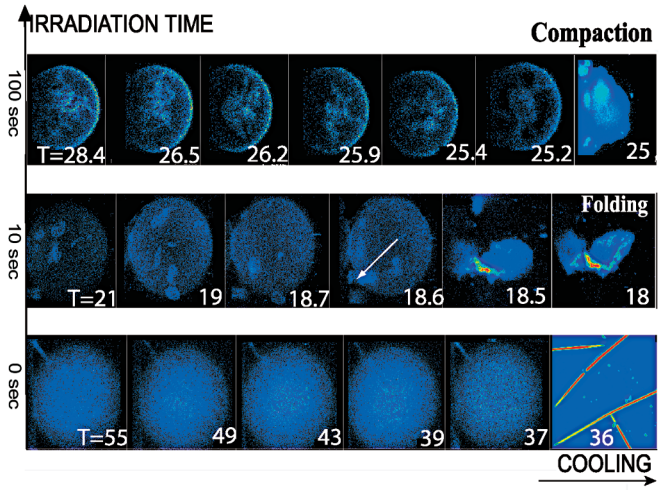

FIG. 1 (color). Two-photon confocal images of vesicles undergoing a wrinkling transformation. The amount of polymerization is measured in time of exposure to uv light. The bottom row shows the formation of cylindrical ribbons at 37 °C for unpolymerized membranes. The middle row represents the folding transformation corresponding to 10 s of exposure (low polymerization) and the transformation occurs at 18 °C. The white arrow points to the location where the domains migrate and where the vesicle ruptures during the wrinkling. The top row represents the wrinkling of a vesicle polymerized for 100 s (No large folds observed). The clear spots are domains (rafts) of polymerized lipids.

With the increase of ϕ, the overall surface features change, and the folds and creases become shallower and smaller, respectively. For 10 μm size vesicles, the creases are on average 500 nm deep for low-polymerization membranes and 20 nm for high-polymerization membranes with an rms ranging from 20 to 5 nm, respectively. The quantitative information of the surface morphology can be extracted from the equal-time height-height correlation function $H(r, t)$ [10], defined as $H(r) = \langle [h(r) - h(0)]^2 \rangle$ where $h(r)$ is the surface height at position $r[= (x, y)]$ on the surface relative to the mean surface height. The notation $\langle \cdots \rangle$ means a spatial average. We report the Fourier transform of $H(r, t)$, or the power spectrum $P(k)$ where k is the wave number. In conjunction with AFM measurements the wrinkled vesicles were observed using an environmental scanning electron microscopy (ESEM) where water vapor is the imaging gas and where no coating is necessary.

The surface of the vesicle is scanned at various regions, a power spectrum is retrieved, and an average is taken. This average is taken for 12 to 15 vesicles. Each vesicle is scanned at various regions and the power spectrum is the average of these scans. The power spectrum is presented in Fig. 2 as well as ESEM images of the wrinkled vesicles. The best fit of the data is a power law of the form $P(k) \sim k^{-\eta}$, where η can be related simply to a roughness exponent in the case of univalued surfaces, depending on ϕ. The amplitude of the folds decreases when the irradiation

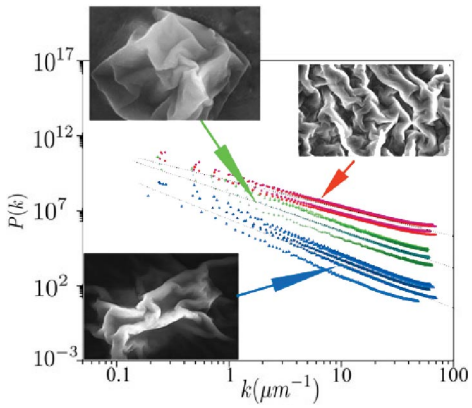

FIG. 2 (color). The power spectrum follows a scaling relation $P(k) \sim k^{-\eta}$. Colors correspond to various irradiation times. The various curves in each color category correspond to different vesicles and different runs. The irradiation times decrease from top to bottom. $\eta \sim 2.00$ for the red curve, which corresponds to a 40% polymerization; $\eta \sim 2.5$ for the green curve, which corresponds to an intermediate polymerization of about 30%; and $\eta \sim 3$ for the blue curve, which corresponds to a 9% polymerization. Insets are ESEM pictures that correspond to the three different phases. The high curving of the plot at high wave number is due to the resolution of the AFM tip. The size of the images is 4 μm.

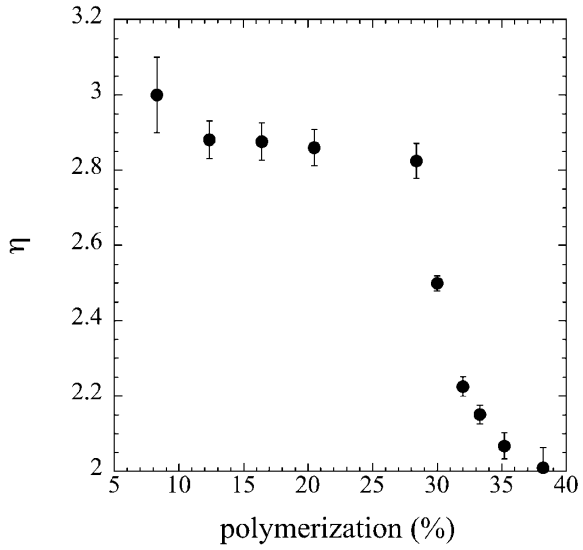

FIG. 3. The η exponent versus polymerization.

time increases, whereupon the amount of polymer produced increases. For $\phi < 30\%$, the surface is smoother at small scales but presents large deformations, and the wrinkling occurs through a succession of folding events. The exponent η is equal to 2.9 ± 0.1. The intermediate region for ϕ between 30% and 32% corresponds to a membrane smoother (at smaller scales) than the fully polymerized one but exhibits a topology that resembles that of a crumpled elastic sheet [1,3], and η is equal to 2.51 ± 0.03. For higher ϕ ($\phi \sim 32\%$ and 40%) the exponent η is equal to 2 ± 0.06 and the surface of the vesicle is rougher at smaller scales and looks like a growth pattern. The folds are of a finer size, surprisingly similar to the ''crumpling'' of metal sheets, where denser foils crumple in denser coils [27]. In Fig. 2 every group of curves (color coded for every polymerization) corresponds to independent experiments and different vesicles. The monodisperse vesicles were taken at random from the solution and scanned. It is evident from these curves that the wrinkled surfaces are statistically equivalent within the same range of polymerization since the power spectrum of every run follows the same power law within 5%–10%. The fact that we have the same power law within the same range of polymerization, where the membrane locks into a similar configuration for this range of polymerization, due in this case to geometrical constraints expressed in terms of the random spontaneous curvature, might be a signature of a glassy phase [18,20,23].

We have systematically investigated the dependence of η versus the amount of polymerization. In Fig. 3, the exponent η of the wrinkled vesicle is constant around the value of 3 over a range of polymerization until a *critical* polymerization of around 28% where it drops to its lowest value of 2 at the percolation threshold. Notice that, at 30%, $\eta \sim 2.5$ similar to the value found for a crumpled elastic sheet [2,28]. The transition at 28% is similar to a supercritical transition where ϕ resembles an order parameter. The membrane is in a mixed flat phase characterized by a roughness exponent equal to 3 over a large range of polymerization, and at a critical value drops abruptly to its lowest value going through an intermediate crumpled phase where the exponent is 2.5. As predicted in [18,29], the locally flat phase, characterized here by $\eta = 3$, spans a certain range in the disorder phase space before the membrane enters a mixed phase, which is characterized here by a short entrance in the crumpled phase after which the exponent drops to 2. At low polymerization, the long-range order responsible for the formation of ribbons is destroyed by the presence of the polymer network. The organization of the membrane into large folds stems from the large deformations the membranes suffer when the ribbons form. When ϕ is increased, the polymer network increases in size and in density (as seen in Fig. 1), which span an area of the order of the radius of curvature of the unpolymerized ribbons. In this case the membrane undergoes a mechanical instability similar to the ribbon formation [30] but of the buckling type whereby the roughness is more sensitive to ϕ. As a last note, in their *tour de force* renormalization group analysis, Radzihovksy and Nelson [21] found that $\langle [h(\mathbf{k})]^2 \rangle \sim k^{-4+\eta_\kappa}$ where η_κ depends on the disorder introduced as a perturbation to the metric of the space embedding the membrane [31].

Contrary to an earlier claim [17,18], the disorder in the form of a polymer network is not quenched in one location of the vesicle but diffuses to different locations. At the

transition to ribbons, the patches, supposedly polymerized in a given curvature, might be in a location where the ribbon will adopt a curvature of different sign. This configuration represents a frustration with respect to ribbons formation, due to the above geometrical constraint. The minimum energy corresponding to the ribbon phase is never achieved, and a wrinkled configuration takes place via a *buckling instability* [19]. The crossover between these three phases is probably due to the appearance of a new length scale or a *correlation length scale* that increases as we increase the polymerization [29]. At low polymerization this correlation scale is of the order of the separation between two lipids' molecules. At higher polymer density, this length scale becomes of the order of the size of the ribbon radius that causes the instability. Another scenario would be that the polymer network is modifying the Gaussian curvature of the membranes, which induces more stretching that balances the pure bending in the absence of polymerization and that creates an instability [32,33].

This work is supported by NSF Grant No. CMS-0238874 and the Grainger Foundation. S. C. thanks D. Bensimon, M. Bowick, G. Gompper, P. Goldbart, L. Radzihovsky, and A. Travesset for fruitful discussions. GP measurements were performed at the Laboratory for Fluorescent Dynamics at the University of Illinois partly supported by the NIH. S. C. thanks the Aspen Center for Physics for hospitality where part of this work took shape.

*Electronic address: sch@uiuc.edu

[1] K. Matan, R. B. Williams, T. A. Witten, and S. R. Nagel, Phys. Rev. Lett. **88**, 076101 (2002).
[2] F. Plouraboué and S. Roux, Physica (Amsterdam) **227A**, 173 (1996).
[3] T. A. Witten and H. Li, Europhys. Lett. **23**, 51 (1993); A. E. Lobkovsky *et al.*, Science **270**, 1482 (1995); A. E. Lobkovsky and T. A. Witten, Phys. Rev. E **55**, 1577 (1997).
[4] M. Benamar and Y. Pomeau, Proc. R. Soc. A **453**, 729 (1997); S. Chaieb, F. Melo, and J. C. Geminard, Phys. Rev. Lett. **80**, 2354 (1998); E. Cerda and L. Mahadevan, Phys. Rev. Lett. **80**, 2358 (1998); E. Cerda *et al.*, Nature (London) **401**, 46 (1999); S. Chaieb and F. Melo, Phys. Rev. E **60**, 6091 (1999).
[5] F. F. Abraham and M. Kardar, Science **252**, 419 (1991).
[6] See *Statistical Mechanics of Membranes and Surfaces*, edited by D. R. Nelson, T. Piran, and S. Weinberg (World Scientific, Singapore, 2004).
[7] M. J. Bowick and A. Travesset, Phys. Rep. **344**, 255 (2001).
[8] T. J. Byers and D. Branton, Proc. Natl. Acad. Sci. U.S.A. **82**, 6153 (1985).
[9] R. R. Chianelli *et al.*, Science **203**, 1105 (1979).
[10] F. F. Abraham and D. R. Nelson, Science **249**, 393 (1990).
[11] G. Grest, J. Phys. I (France) **1**, 1695 (1991).
[12] M. J. Bowick *et al.*, Eur. Phys. J. E **5**, 149 (2001).
[13] C. F. Schmidt *et al.*, Science **259**, 952 (1993).
[14] T. Hwa, E. Kokufuta, and T. Tanaka, Phys. Rev. A **44**, R2235 (1991); X. Wen *et al.*, Nature (London) **355**, 426 (1992).
[15] M. S. Spector, E. Naranjo, S. Chiruvolu, and J. A. Zasadzinski, Phys. Rev. Lett. **73**, 2867 (1994).
[16] M. Mutz, D. Bensimon, and M. J. Brienne, Phys. Rev. Lett. **67**, 923 (1991).
[17] D. Bensimon, D. Mukamel, and L. Peliti, Europhys. Lett. **18**, 269 (1992).
[18] R. Attal, S. Chaieb, and D. Bensimon, Phys. Rev. E **48**, 2232 (1993).
[19] D. R. Nelson and L. Radzihovsky, Phys. Rev. A **46**, 7474 (1992).
[20] D. R. Nelson and L. Radzihovsky, Europhys. Lett. **16**, 79 (1991).
[21] L. Radzihovsky and D. R. Nelson, Phys. Rev. A **44**, 3525 (1991).
[22] D. C. Morse, T. C. Lubensky, and G. S. Grest, Phys. Rev. A **45**, R2151 (1992); D. C. Morse and T. C. Lubensky, *ibid.* **46**, 1751 (1992).
[23] G. D'Anna and G. Gremaud, Nature (London) **413**, 407 (2001); C. S. O'Hern, S. A. Langer, A. J. Liu, and S. R. Nagel, Phys. Rev. Lett. **86**, 111 (2001); B. Chakraborty, D. Das, and J. Kondev, Eur. Phys. J. E **9**, 227 (2002).
[24] J. V. Selinger, M. S. Spector, and J. M. Schnur, J. Phys. Chem. **105**, 7157 (2001).
[25] B. N. Thomas, C. M. Lindemann, and N. A. Clark, Phys. Rev. E **59**, 3040 (1999).
[26] T. Parasassi *et al.*, J. Fluoresc. **8**, 365 (1998). The density of Laurdan molecules is small enough (1 molecule in 200 lipid molecules) that the mechanical properties of the vesicles, made of pure lipids, are not affected. The emission spectrum of Laurdan is shifted as the amount of water around its headgroup varies. It is a good indicator for the melting transition and the thermodynamics state of the membrane. The transition from spherical fluctuating vesicle to a helical ribbon might not be ''strictly'' a transition from a gel to liquid crystalline state but would correspond to change in the packing of the molecules at the melting temperature. Above T_m the lipid molecules fluctuate, and below T_m they are closely packed and do not fluctuate.
[27] M. A. F. Gomes *et al.*, J. Phys. D **22**, 1217 (1989).
[28] D. L. Blair and A. Kudrolli, Phys. Rev. Lett. **94**, 166107 (2005).
[29] L. Radzihovsky and P. Le Doussal, J. Phys. I (France) **2**, 599 (1992); P. Le Doussal and L. Radzihovsky, Phys. Rev. B **48**, R3548 (1993).
[30] J. V. Selinger, F. C. MacKintosh, and J. M. Schnur, Phys. Rev. E **53**, 3804 (1996).
[31] They considered a phantom membrane where $\eta_\kappa = (A - \sigma_1 - \sigma_2[B + C])$ where σ_1 and σ_2 are ''measures'' of the disorder in the metric and A, B, and C are nondimensional elastic constants.
[32] Y. Pomeau, Philos. Mag. B **78**, 235 (1998).
[33] S. Schneider and G. Gompper, Europhys. Lett. **70**, 136 (2005).